International Journal of Women's Health

Dovepress
Taylor & Francis Group

Open Access Full Text Article

ORIGINAL RESEARCH

Study on Differential Metabolites Between Human Papillomavirus Infection and Cervical Cancer Based on Non-Targeted Metabolomics

Jinmei Xu, Ming Wang, Yue Jia, Yanfen Chen, Yangjuan Duan, Mengting Ni, Yinghai Wang, Jie Wei, Jing Yu

Department of Gynecology, The Third Affiliated Hospital of Kunming Medical University, Yunnan Cancer Hospital, Peking University Cancer Hospital Yunnan, Kunming, Yunnan, 650118, People's Republic of China

Correspondence: Jing Yu, Email 774878940@qq.com

Objective: To explore the difference of metabolites between human papillomavirus (HPV) infection and the occurrence and development of cervical cancer based on non-targeted metabolomics.

Methods: Between August 2022 and August 2023, 20 women of childbearing age at the Third Affiliated Hospital of Kunming Medical University, including the HPV-negative control, LSIL (HPV infection), HSIL (cervical intraepithelial neoplasia [CIN2-3]), and cervical cancer groups, were selected as research participants. Ultra-high-performance liquid chromatography and SCIEX mass spectrometry (TripleTOF 6600+, USA) were used to separate and detect the metabolites.

Results: According to the results of the differential metabolite analysis, the KEGG pathway was enriched. The most obvious enrichment pathway in the CIN2-3 group compared with the HPV-negative and HPV-positive groups was the steroid hormone pathway; the most obvious enrichment pathway in the cervical cancer group compared with the HPV-negative group was the steroid hormone pathway. Compared with HPV-negative group, the most obvious enrichment pathway in the CIN2-3 group was the glycerophosphate metabolism pathway. Compared with CIN2-3 and HPV-positive group, the most obvious enrichment pathway in the cervical cancer group was the sphingolipid metabolism pathway, followed by the steroid biosynthesis and amino sugar and nucleotide metabolism pathways. Compared with the HPV-negative group, the most obvious enrichment pathway in the cervical cancer group was the steroid biosynthesis pathway, followed by the sphingolipid metabolism pathway. 19-Hydroxytestosterone is involved in the synthesis of steroid hormones. Cerebroside B is involved in sphingolipid metabolism. Potassium acetate is involved in protein digestion and absorption. Methylarsonate is involved in chemical carcinogenesis - reactive oxygen species.

Conclusion: The expression levels of 19-Hydroxytestosterone, cerebroside B, potassium acetate and methylarsonate are down-regulated with the aggravation of cervical lesions and can be used as potential tumor markers for cervical cancer.

Keywords: cervical cancer, non-targeted metabolomics, HPV

Introduction

Cervical cancer is the fourth most common cancer in women worldwide. The burden faced by low- and middle-income countries was greater than that faced by high-income countries.[1] More than 90% of cervical cancers are caused by human papillomavirus (HPV) infection, which leads to cervical intraepithelial neoplasia (CIN)1/2/3, eventually leading to invasive cervical cancer. Active monitoring of CIN2 without treatment increases the long-term risk of cervical cancer, and treatment of precancerous lesions can prevent > 90% of cancers.[2,3] Therefore, the early screening and detection of cervical lesions are important for the prevention and treatment of cervical cancer. HPV infection is one of the most common sexually transmitted infections worldwide.[4] HPV-infected cells also affect the local environment and create a supportive postinfection microenvironment, which is gradually being recognized as a key factor in the persistence, spread, and malignant progression of the virus.[5]

Received: 18 February 2025
Accepted: 17 October 2025
Published: 30 October 2025

Many efforts have been made worldwide to eradicate cervical cancer, including improved disease screening and HPV vaccination programs. Persistent infection with high-risk HPV genotypes 16 and 18 is the main cause of cancer, and may lead to HPV integration into the host genome.[6] The female genital tract is similar to other mucosal parts of the body, and contains specific microbial groups that are usually dominated by Lactobacillus (spp). Cross-sectional and longitudinal studies have reported that the consumption of Lactobacillus increases with the severity of CIN, and that the microbial composition owing to Lactobacillus consumption may lead to a pro-inflammatory environment, thus increasing the proliferation of malignant cells and the expression of HPV E6 and E7 oncogenes.[7] Inhibiting the activity of the E6 and E7 oncoproteins may be a better selective target for delaying the progression of cervical cancer.[8] Persistent infection with the high-risk HPV (HR-HPV) remains a primary risk factor for cervical cancer. HPV genotyping of HPV-positive patients with normal cytological examination results or HSIL can accelerate the management of a considerable proportion of patients with abnormal test results.[9] Non-targeted metabonomic can non-biasedly detect and quantify all metabolites in the sample. However, some patients still develop cervical cancer directly without HPV infection. Therefore, we hope to provide more sensitive biomarkers for the diagnosis of cervical cancer through metabonomic research. Cervical cancer can exist in a precancerous state for many years, and research on the microorganisms involved in cervical cancer will enhance our understanding of the interference of viral host cells and the occurrence and progression of cervical cancer.

We found that the overexpression of human hydroxysteroid dehydrogenase-like protein 2 (HSDL2) was related to the progression of cervical cancer, including lymph node metastasis and recurrence. Thus, HSDL2 can be used as a new marker for the early diagnosis of cervical cancer. HSDL2 also initiates and promotes the proliferation, invasion, and migration of cervical cancer cells (HeLa, C33A, and SiHa) through Epithelial-mesenchymal transition (EMT), thus promoting the occurrence of tumors. In addition, HSDL2 is involved in the occurrence of tumors by regulating lipid metabolism.[10]

Metabolomics analyses of biological samples from patients with HPV-negative, high-risk HPV persistent infection, CIN, and cervical cancer are helpful to clarify the pathway of occurrence and development of cervical cancer and identify metabolites and pathways related to HPV infection and CIN.

Materials and Methods

Participants and Grouping

Between August 2022 and August 2023, 80 women of childbearing age at the Third Affiliated Hospital of Kunming Medical University were computerized randomization as research participants. According to the results of cervical pathology, the participants were divided into HPV-negative control (HPVyin group), LSIL (HPVyang group), HSIL (CIN2-3), and cervical cancer groups (GJA group), with 20 cases per group. Secretion samples from the posterior vaginal vault of the participants were collected and placed in sterile test tubes for metabolite detection. The inclusion criteria were as follows: (1) female patients of childbearing age who were not yet menopausal; (2) no history of using hormonal drugs; (3) cervical lesions confirmed by pathology; and (4) participants in the follicular phase (within 7 days of clean menstruation). Exclusion criteria were as follows: (1) use of vaginal antibacterial drugs, sexual intercourse, or vaginal irrigation in the last 2 days; (2) inflammation such as clue cells, fungi, trichomonas, and Chlamydia infection detected in vaginal secretions; (3) gonorrhea, syphilis, AIDS, genital herpes, and other sexually transmitted diseases; (4) history of cervical treatment or total hysterectomy; and (5) history of systemic diseases such as endocrine and metabolic diseases, autoimmune diseases, and other malignant tumors. The average ages of the HPV-negative control, LSIL (HPV infection), HSIL (CIN2-3), and cervical cancer group were 39.75 ± 7.566, 35.20 ± 6.429, 35.25 ± 4.962, and 38.25 ± 7.608 years, respectively, with no statistical significance (F=2.265). This study was approved by the Hospital Ethics Committee of the Third Affiliated Hospital of Kunming Medical University and all participants provided informed consent.

Methods

Sample Collection

A sterile vaginal swab was used to collect secretions at the vaginal vault and the swab was rotated in the vagina for 10–15 s to ensure full absorption of secretions. Each swab was carefully placed in a sterile dry test tube to prevent sample

contamination. The patient information and number on the tube wall were marked to ensure that the samples were not confused. The samples were immediately placed into a −80 °C refrigerator for storage.

Sample Extraction

The sample was removed from the refrigerator at −80 °C and slowly thawed on ice. Then the sample was transferred to a new centrifuge tube, a mixed solvent of 20% acetonitrile and 80% methanol was added, along with an internal standard. The sample was mixed in a vortex for 3 min and treated ultrasonically for 10 min. After centrifugation at 12000 rpm for 10 min, the solid and liquid phases of the extract were separated. The supernatant was collected and concentrated to dryness. The dried metabolites were redissolved in a 70% methanol aqueous solution and centrifuged again at 12000 rpm for 3 min to remove insoluble substances. The supernatant was transferred to a sampling bottle for mass spectrometry or chromatographic analysis.

Chromatographic and Mass Spectrometry Analysis

In this experiment, ultra-high-performance liquid chromatography (LC-30A Japan) and a SCIEX mass spectrometer (TripleTOF 6600+, USA) were used to separate and detect the metabolites, and an AB TripleTOF 6600 mass spectrometer was used to detect the metabolites.

Data Processing and Statistical Methods

The originally collected data collected was pre-processed using a mass spectrometer. Metabolite identification was performed by searching a database built by the laboratory, integrating the public database, AI prediction database, and the metDNA method. The samples were randomly sorted, and every ten samples were interspersed with one quality control (QC) sample. The MetaboAnalystR package in the R software was used to analyze differential metabolites. The clinical data of the participants were analyzed using One-way analysis of variance by the IBM SPSS software (version 26.0), $P < 0.05$ suggesting that the difference was statistically significant.

Results

Sample Quality Control Analysis

By overlapping and displaying the total ion current (TIC) diagram of different QC samples, we judged the repeatability of metabolite extraction and detection, that is, technical repetition was performed. The high stability of the instrument provides an important guarantee of the repeatability and reliability of the data. As shown in Figure 1, the separation effect of each chromatographic peak is good, the number of peaks is large, and the corresponding intensity is high, indicating that the experimental analysis conditions met the analysis requirements of metabolomics, the serum quality sample met the experimental requirements, and the mass spectrum signal was stable.

Cluster Analysis

To express the differential metabolites and clustering relationship between samples, the expression levels of metabolites in the samples were represented by color and depth. As shown in Figure 2. Firstly, the data were standardized by unit variance scaling, and all samples were analyzed by cluster heat map; the cluster heat map was drawn using an R program script. Samples were clustered vertically and each group of samples was clustered horizontally. The figure shows the differences in the contents of the top 26 types of substances among the four groups (20 per group).

Principal Component Analysis

Through principal component analysis of the samples, including QC samples, Figure 3 revealed clear discrimination between groups and good repeatability within each group.

Orthogonal Partial Least Squares Discriminant Analysis

Orthogonal Partial Least Squares Discriminant Analysis Score Chart

In this study, the Orthogonal partial least squares discriminant analysis (OPLS-DA) was used to screen the differential metabolites. As shown in Figure 4A–F, significant differences were observed between the CIN2-3 and HPV-infected

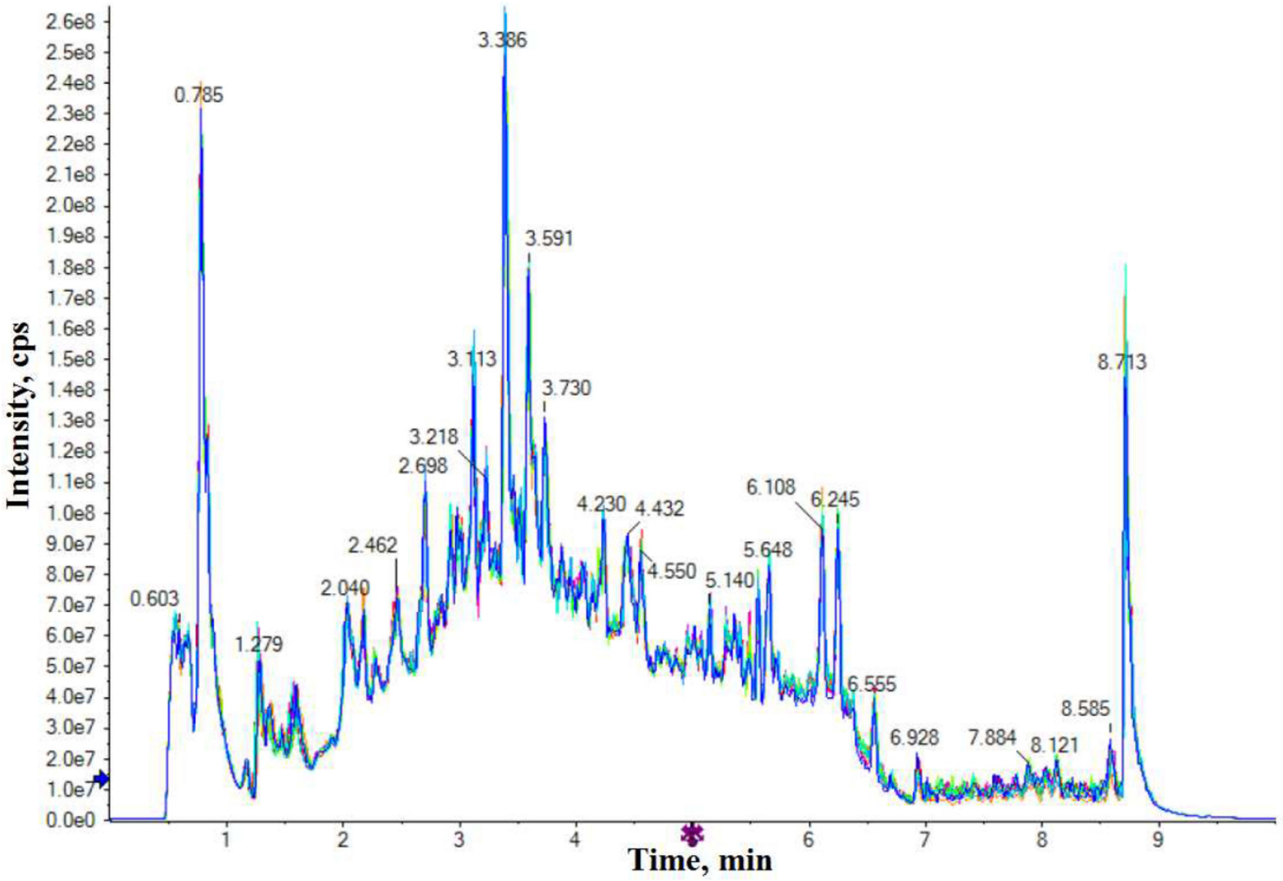

Figure 1 Overlaid Total Ion Chromatogram (TIC) of QC Sample Mass Spectrometry Detection.

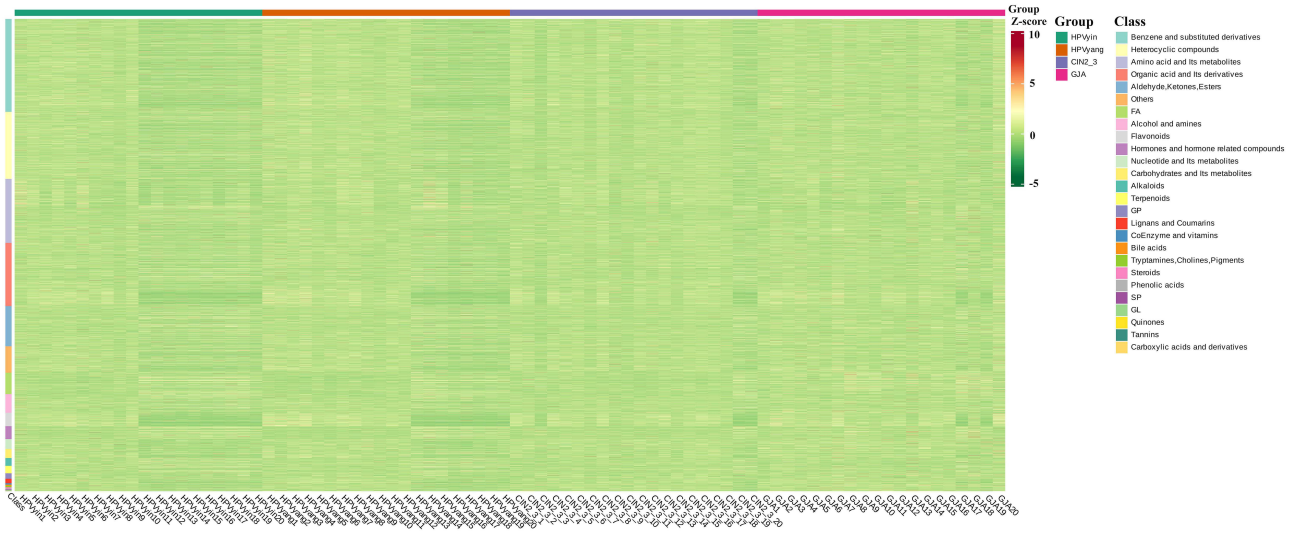

Figure 2 Heatmap of Overall Sample Clustering.

groups (Figure 4A), CIN2-3 and HPV-negative groups (Figure 4B), cervical cancer and HPV-infected groups (Figure 4D), cervical cancer and HPV-negative groups (Figure 4E), and HPV-negative and HPV-infected groups (Figure 4F), which indicated that the differential metabolites preliminarily screened in this study were reliable.

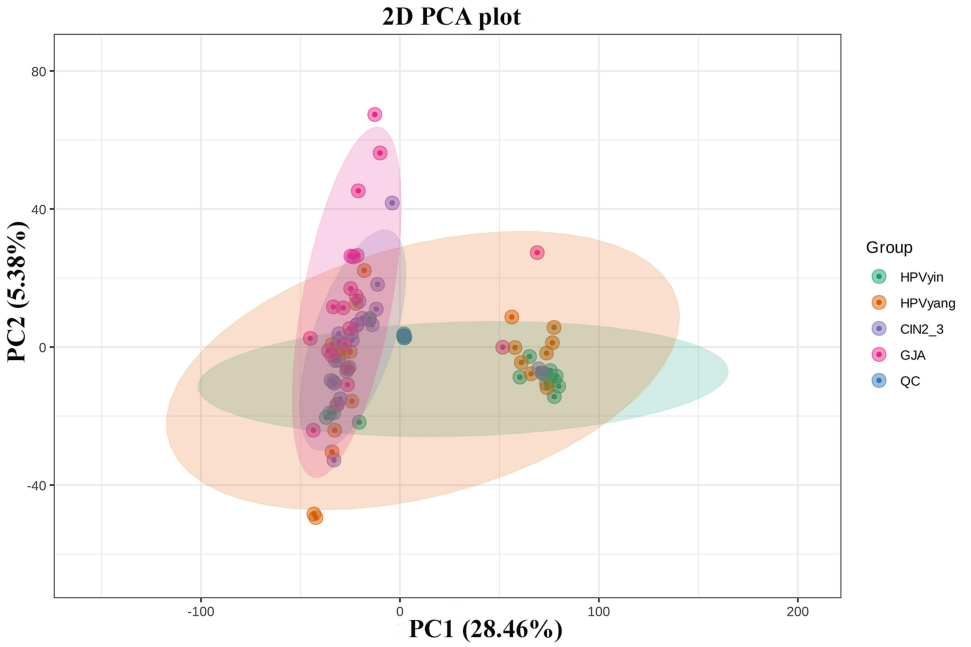

Figure 3 Principal Component Analysis (PCA) Score Plot. PC1 represents the first principal component, and PC2 represents the second principal component, and so on. The percentage indicates the contribution of each principal component to the sample differences. Each point in the plot represents a sample, with samples from the same group indicated by the same color. If a group contains more than three samples, an elliptical confidence interval is added. Confidence intervals can also be added for groups with exactly three samples if necessary.

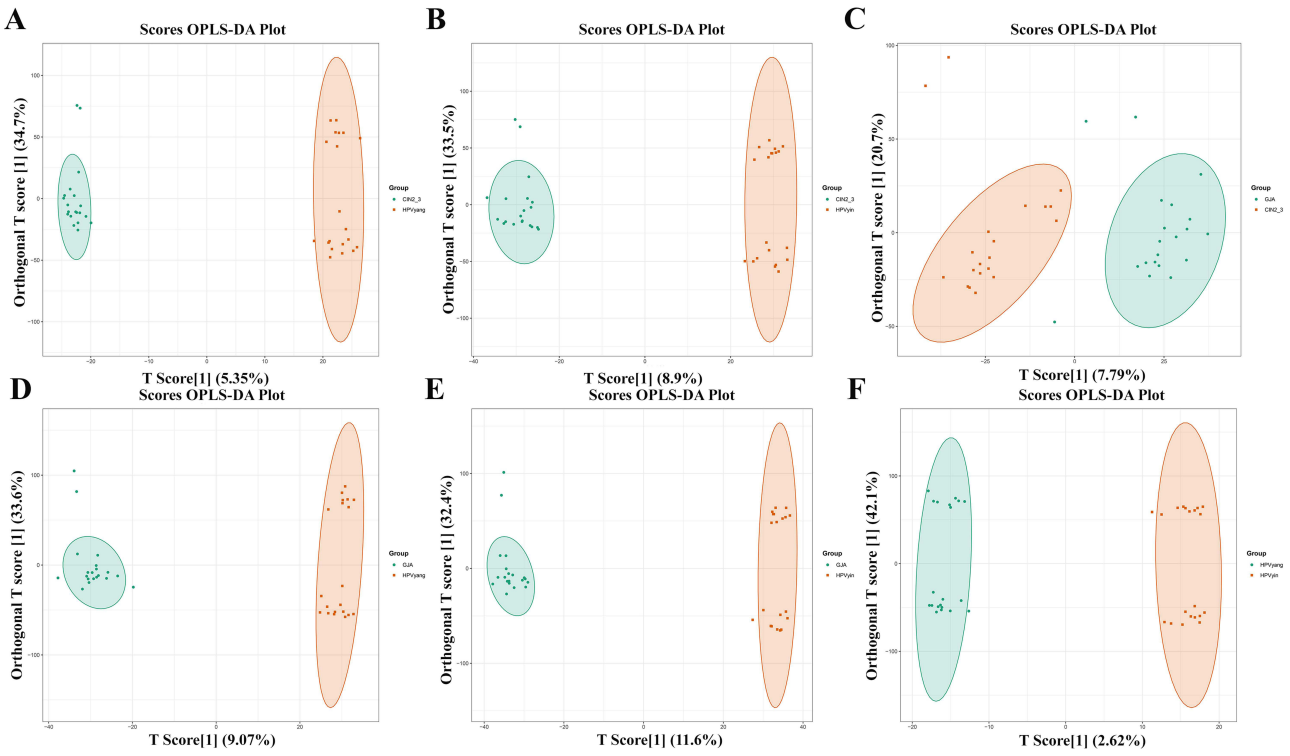

Figure 4 Orthogonal Partial Least Squares Discriminant Analysis (OPLS-DA) Score Plot (**A**) CIN2-3 groups vs HPVyang groups; (**B**) CIN2-3 groups vs HPVyin groups; (**C**) GJA groups vs CIN2-3 groups; (**D**) GJA groups vs HPVyang groups; (**E**) GJA groups vs HPVyin groups; and (**F**) HPVyang groups vs HPVyin groups. The x-axis represents the predictive component score, reflecting the differences between sample groups. The greater the distance on the x-axis, the more significant the differences between groups. The y-axis represents the orthogonal component score, reflecting the variability within groups. The percentage indicates the explained variance of the principal components of the differential metabolites in the dataset.

https://doi.org/10.2147/IJWH.S523559

OPLS-DA Model Verification

Figure 5A–F shows the OPLS-DA verification chart, where the abscissa represents the values of R2Y and Q2 of the model, and the ordinate is the frequency of the model classification effect; that is, this model has conducted 200 random permutation and combination experiments on the data, and the Figure 5A–F Q2 is $P< 0.05$, which shows zero random grouping models with better prediction ability than the OPLS-DA model in this permutation detection. In Figure 5A, a $P = 0.085$ in R2Y shows 17 random grouping models in this permutation detection, and the interpretation rate of the Y matrix was better than that of the OPLS-DA model. $P = 0.01$ in Figure 5B, R2Y shows two random grouping models in this permutation detection, and the interpretation rate of the Y matrix was better than that of the OPLS-DA model. In Figure 5C, a $P = 0.055$ in R2Y shows 11 random grouping models in this permutation detection, and the interpretation rate of the Y matrix was better than that of the OPLS-DA model. In Figures 5D and E, a $P < 0.005$ in R2Y shows zero random grouping models in this permutation test, and the interpretation rate of the Y matrix is better than that of the OPLS-DA model. In Figure 5F, a $P = 0.09$ in R2Y shows 18 random grouping models in this permutation detection, and the interpretation rate of the Y matrix was better than that of the OPLS-DA model. In general, the model was considered the best when $P < 0.05$.

Screening of Differential Metabolites

Based on the variable importance in projection (VIP) obtained from OPLS-DA model (biological repetition ≥ 3), the metabolites with differences among different tissues were preliminarily screened. In this study, metabolites with VIP > 1 and $P < 0.05$ were selected as differential metabolites.

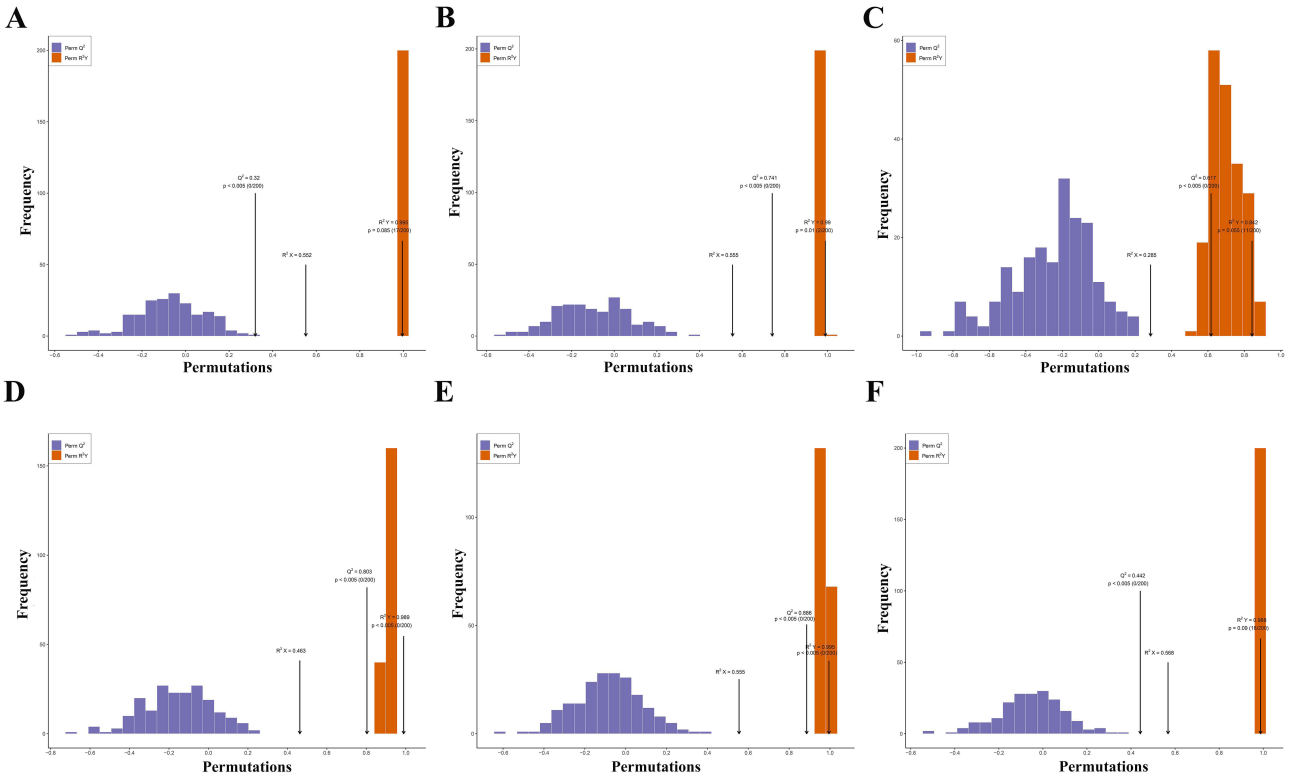

Figure 5 OPLS-DA Validation Plot (**A**) CIN2-3 groups vs HPVyang groups; (**B**) CIN2-3 groups vs HPVyin groups; (**C**) GJA groups vs CIN2-3 groups; (**D**) GJA groups vs HPVyang groups; (**E**) GJA groups vs HPVyin groups; and (**F**) HPVyang groups vs HPVyin groups. The x-axis represents the model RY and Q values, while the y-axis shows the frequency of classification effects in 200 random permutation tests. The Orange color represents the RY values of the random grouping model, and the purple color represents the Q values of the random grouping model. The black arrow indicates the original model's RX, RY, and Q values.

Table 1 Statistical Table of the Number of Differential Metabolites

Graph	Group	Total	Down	Up
a	CIN2_3_vs_HPVyang	1001	646	355
b	CIN2_3_vs_HPVyin	2602	1846	756
c	GJA_vs_CIN2_3	1470	988	482
d	GJA_vs_HPVyang	2449	1639	810
e	GJA_vs_HPVyin	3322	2309	1013
f	HPVyang_vs_HPVyin	591	510	81

Volcano Plots of Differential Metabolites

In this study, 80 samples were selected and divided into four groups for metabolic analysis. A total of 11435 metabolites were detected, with 3497 showing increased levels and 7938 showing decreased levels. As shown in Table 1 and Figure 6A–F.

VIP Value Chart of Differential Metabolites

The top 20 metabolites with the largest VIP value in the OPLS-DA model were selected to show the differential metabolites identified based on screening criteria in each group comparison. As shown in Figure 7A–F. Compared with the HPV-negative group, most of the glycerophosphates in other groups showed an upward trend, and with the aggravation of the disease, the glycerophosphates showed a downward trend. Fatty acyl groups showed an upward trend in the cervical cancer and CIN2-3 groups (Figure 7D), and a downward trend in the other groups. Nucleotides and their metabolites showed an upward trend in most groups. Organic acids and their derivatives, amino acids and their metabolites, sphingolipids, glycerols, alcohols, and amines showed decreasing trends for each group. Benzene and its derivatives, aldehydes, ketones, and esters showed a downward trend in most groups.

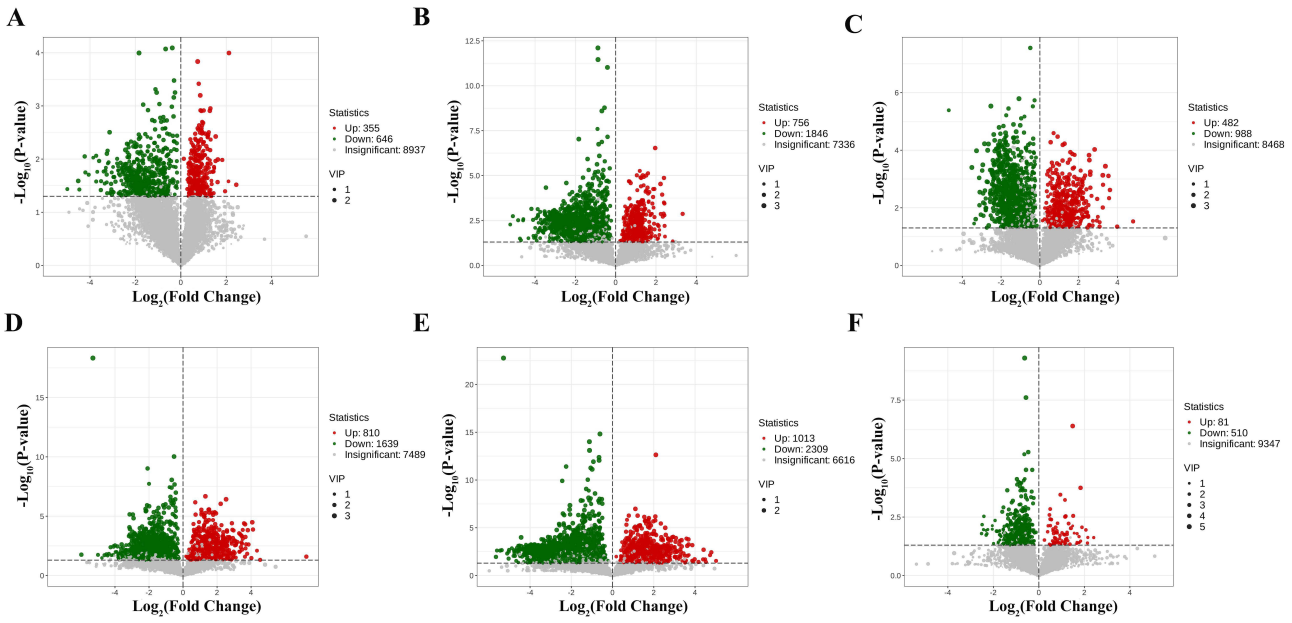

Figure 6 Volcano Plot of Differential Metabolites (**A**) CIN2-3 groups vs HPVyang groups; (**B**) CIN2-3 groups vs HPVyin groups; (**C**) GJA groups vs CIN2-3 groups; (**D**) GJA groups vs HPVyang groups; (**E**) GJA groups vs HPVyin groups; and (**F**) HPVyang groups vs HPVyin groups. Each point represents a metabolite, with green indicating downregulation and red indicating upregulation. Gray points represent metabolites detected but with non-significant differences. The x-axis represents the logarithm of the fold change in relative abundance between the two groups of samples. The greater the absolute value on the x-axis, the larger the difference in relative abundance between the two groups. The y-axis represents the significance level of the differences, with the size of the dots representing the VIP value.

https://doi.org/10.2147/IJWH.S523559

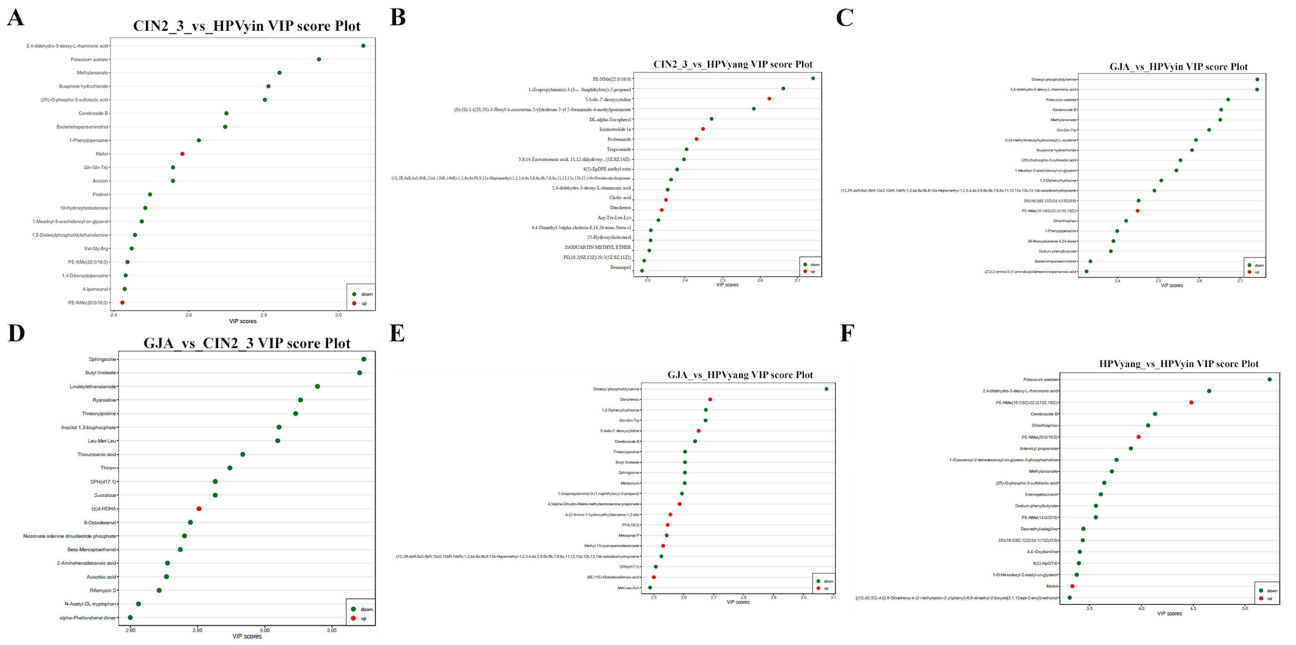

Figure 7 VIP Value Plot of Differential Metabolites (**A**) CIN2-3 groups vs HPVyin groups; (**B**) CIN2-3 groups vs HPVyang groups; (**C**) GJA groups vs HPVyin groups; (**D**) GJA groups vs CIN2-3 groups; (**E**) GJA groups vs HPVyang groups; and (**F**) HPVyang groups vs HPVyin groups. The x-axis represents the VIP value, while the y-axis represents the differential metabolites. Red indicates upregulated metabolites, green indicates downregulated metabolites, and yellow represents metabolites that are significantly different in comparisons involving three or more groups.

Enrichment Analysis of KEGG Pathway of Differential Metabolites

According to the results of the differential metabolites, the KEGG pathway was enriched, where the Rich Factor was the ratio of the number of differential metabolites in the corresponding pathway to the total number of metabolites annotated in the pathway; the greater the value, the greater was the enrichment degree. The sizes of the dots in the graph represent the number of significantly different metabolites enriched in the corresponding pathways. As shown in Figure 8A–F. The top 20 pathways by P-value were selected for display from small to large: we find that show pathway the steroid hormone is the most important pathway in the CIN2-3 group compared with the HPV-negative and HPV-positive groups (Figure 8A and B), the amino sugar and nucleotide sugar metabolism pathways was is the most important pathway in the cervical cancer group compared with the CIN2-3 and HPV-positive groups (Figure 8C and D), the steroid hormone pathway was is the most important pathway in the cervical cancer group compared with the HPV-negative group (Figure 8E), and the Kaposi sarcoma-related herpesvirus infection pathway was is the most important pathway in the HPV-positive and HPV-negative groups (Figure 8F).

Metabolite Set Enrichment Analysis (MSEA)

To avoid missing metabolites with insignificant differential expression but important biological significance, we conducted MSEA. As shown in Figure 9A–F. The top 50 metabolic sets were selected by p-values for MSEA enrichment analysis. Compared with the HPV-positive group, we find that enrichment pathways in the CIN2-3 group were ascorbic acid and aldonic acid metabolic pathways and phosphatidylinositol signaling pathway (Figure 9A). Compared with HPV-negative group, the most obvious enrichment pathway in the CIN2-3 group was the glycerophosphate metabolism pathway (Figure 9B). Compared with CIN2-3 group and HPV-positive group, the most obvious enrichment pathway in the cervical cancer group was the sphingolipid metabolism pathway, followed by the steroid biosynthesis and amino sugar and nucleotide metabolism pathways (Figure 9C and D). Compared with the HPV-negative group, the most obvious enrichment pathway in the cervical cancer group was the steroid biosynthesis pathway, followed by the sphingolipid metabolism pathway (Figure 9E). Compared to the HPV-negative group, nicotinic acid and nicotinamide

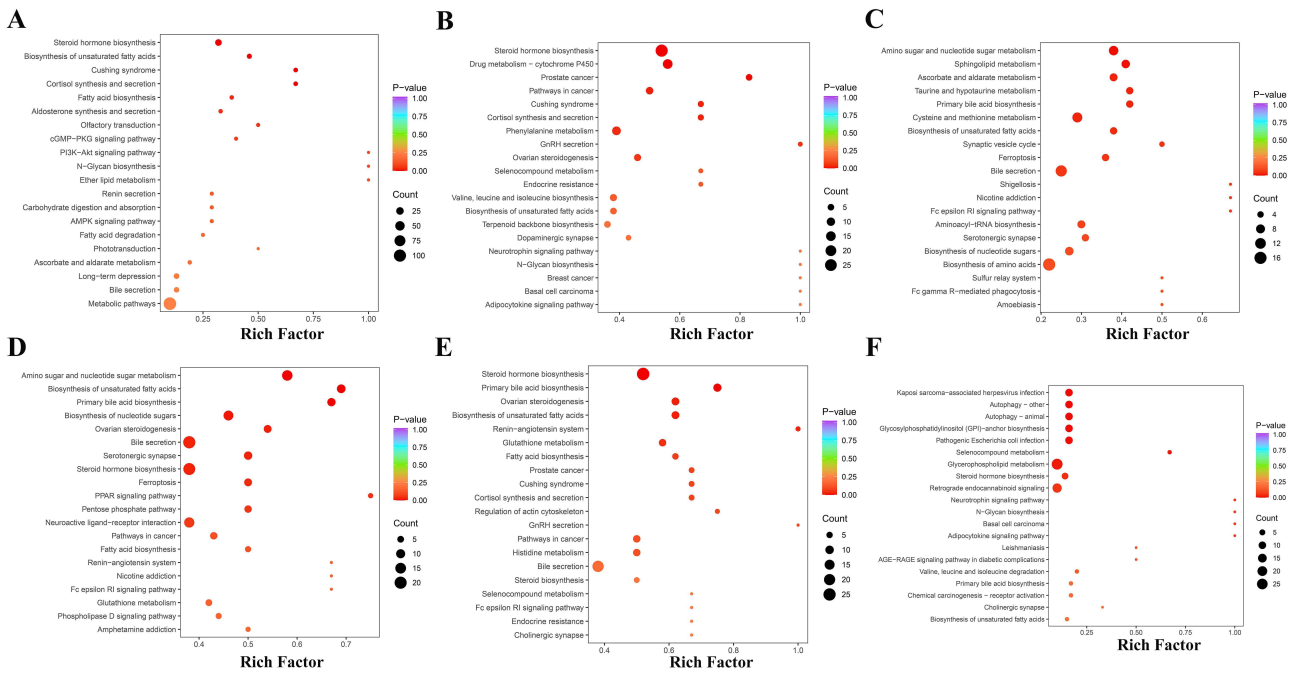

Figure 8 KEGG Enrichment Plot of Differential Metabolites (**A**) CIN2-3 groups vs HPVyang groups; (**B**) CIN2-3 groups vs HPVyin groups; (**C**) GJA groups vs CIN2-3 groups; (**D**) GJA groups vs HPVyang groups; (**E**) GJA groups vs HPVyin groups; and (**F**) HPVyang groups vs HPVyin groups. The x-axis represents the enrichment degree for each pathway, while the y-axis lists the pathway names (sorted by P-value). The color of the points indicates the P-value, with redder colors indicating more significant enrichment. The size of the points represents the number of differential metabolites enriched in each pathway.

metabolic pathways were the most enriched in the HPV-positive group, followed by the glycerophosphate metabolic pathway (Figure 9F).

Differential Metabolite Analysis

For the differential metabolites identified based on the screening criteria in each group comparison, the top 20 metabolites with the highest VIP values in each group of the OPLS-DA model were selected for pathway screening analysis. Eventually, 4 substances with statistically significant differences and clear metabolic pathways in each group were screened out, which can be used as tumor markers for the cervix. Among them, 19-Hydroxytestosterone is involved in Steroid hormone biosynthesis. Cerebroside B belongs to GSP and is involved in Sphingolipid metabolism. Potassium acetate is involved in Protein digestion and absorption. Methylarsonate is involved in Chemical carcinogenesis - reactive oxygen species. As shown in Figure 10A–D, these four types of substances decrease with the aggravation of the lesion ($P < 0.05$), and the differences are statistically significant. They are closely related to the occurrence and development of cervical cancer and can be used as tumor markers for cervical cancer.

Discussion

HPV Infection and Metabolomics

The vast majority of cervical cancers are mainly caused by persistent HR-HPV infection, and approximately 95% of cervical cancers are HPV-positive.[11] HR-HPV causes epithelial basal cell dysfunction, leading to cervical cancer.[12] Metabolites are the final products of various biological processes.[13] Therefore, in this study, we aimed to identify reliable biomarkers of HPV infection by studying cervical and vaginal metabolites. Moreover, metabolites of reduced glutathione (GSH) and oxidized glutathione (GSSG) in HPV-positive women are lower than those in HPV-negative women. In addition, lipid glyceryl choline (33.6%), 3-hydroxydecanoate (33.9%), and choline phosphate (73.7%) levels were lower in women with HPV.[14] Ilhan et al (2019) showed[15] that compared with the HPV (-) group, the HPV (+), LSIL, and HSIL groups mainly consumed metabolites in the amino acid pathway. The metabolites in the HPV (+) group were mainly consumed during lysine, polyamine, and phenylalanine metabolism. Zhang et al showed[16] that the different metabolites

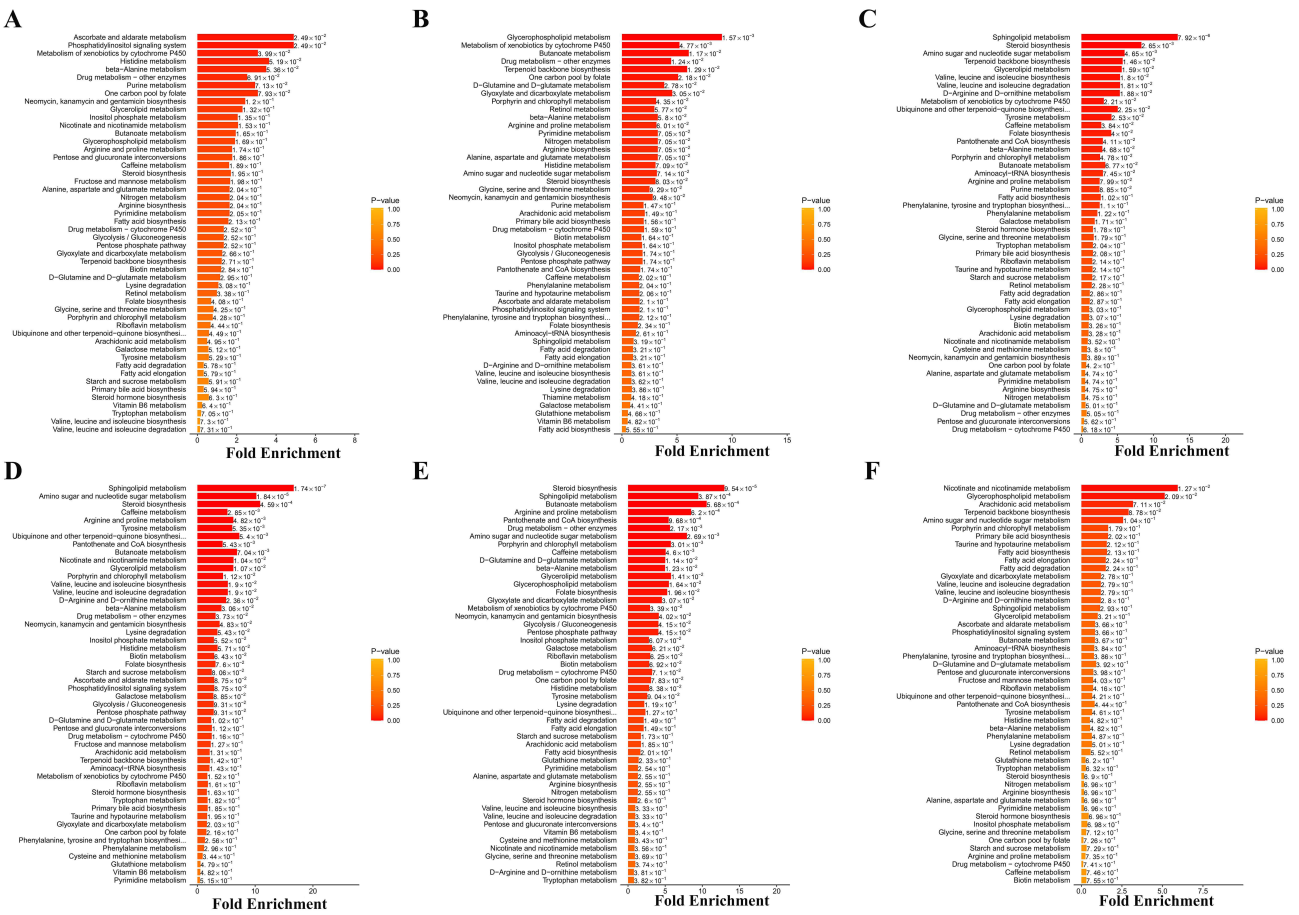

Figure 9 MSEA Enrichment Analysis Plot (**A**) CIN2-3 groups vs HPVyang groups; (**B**) CIN2-3 groups vs HPVyin groups; (**C**) GJA groups vs CIN2-3 groups; (**D**) GJA groups vs HPVyang groups; (**E**) GJA groups vs HPVyin groups; and (**F**) HPVyang groups vs HPVyin groups. The y-axis represents the names of the metabolic sets (sorted by P-value), with corresponding P-values annotated. The x-axis represents the fold enrichment. The color indicates the P-value, with colors closer to red (P-value closer to 0) indicating more significant enrichment.

between normal and HPV groups included linolenic acid, glycerophosphate, and arachidonic acid metabolism; unsaturated fatty acid biosynthesis; lysine degradation; pyruvate metabolism; and primary cholecystic acid biosynthesis. Using the urine samples of the Puerto Rican woman followed by GC-MS analysis we have shown, that patients with high-risk HPV infections have the significantly higher abundance of 5-Oxoprolinate, Erythronic acid, and N-Acetylaspartic acid.[17] Our study revealed that the metabolic pathways of nicotinic acid, nicotinamide, and glycerophosphate are closely related to HPV infection.

Cervical Precancerous Lesions and Metabolomics

Cervical cancer is one of the most common malignant tumors in women worldwide. HR-HPV infection usually takes a long time to develop into cervical cancer. CIN is an important precancerous lesion of cervical cancer. The development of cancer from normal cervical tissue is a continuous process.[18,19] Therefore, we not only need to prevent and monitor the development of normal cervical tissues or cells to CIN, but also treat and block the development of CIN in cervical cancer. Therefore, in this study, we aimed to identify reliable biomarkers for the diagnosis and treatment of CIN by studying the cervical and vaginal metabolites of CIN. Previous studies have shown that the metabolic spectrum can clearly distinguish cervical precancerous lesions from the normal cervical epithelium and cervical cancer. Compared to the normal cervical epithelium, glucose consumption and lactic acid secretion were increased in cervical precancerous lesions. The expression of the glycolytic enzymes pyruvate kinase M2 (PKM2), lactate dehydrogenase (LDHA), hexokinase II (HKII) in cervical precancerous lesions tends to be higher than that in the normal cervical epithelium;

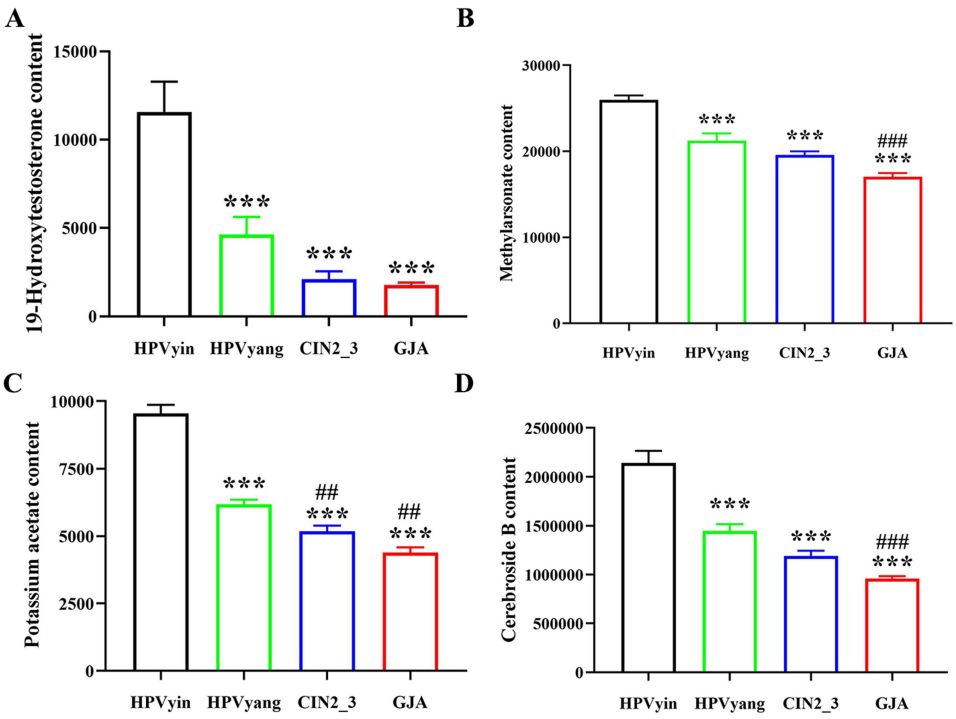

Figure 10 The expression level of differential metabolites among different Groups. (**A**) 19-Hydroxytestosterone; (**B**) Methylarsonate; (**C**) Potassium acetate, and (**D**) Cerebroside B. N=20, ***$P<0.001$ vs HPVyin groups; ##$P<0.01$, ###$P<0.001$vs HPVyang groups.

there is increased glucose consumption and lactic acid production in precancerous cervical lesions.[20] This study found that PE-NMe (20:0/16:0) increased in the CIN2-3 group, whereas 19-Hydroxytestosterone, Cerebroside B, Potassium acetate and Methylarsonate, diglyceride, and PE-NMe (22:0/16:0) decreased in the CIN2-3 group. This indicates that these are closely related to the occurrence and development of cervical cancer. Compared with the HPV-negative and HPV-positive groups, the most obvious enrichment pathways in the CIN2-3 group were the steroid hormone and glycerophosphate metabolism pathways. This indicated that lipid metabolism plays an important role in cervical cancer development.

Cervical Cancer and Lipid Metabolism

Lipids are the main components of the cell membrane and the main energy suppliers, and are involved in signal transduction. Lipids not only contain fatty acids but also include several other functional variants, such as alcohols, aldehydes, amines, and esters.[21] Different types of glycerophospholipids, including phosphatidylcholine and phosphatidylethanolamine, form a metabolic network controlled by various enzymes. Phosphatidylcholine can be deacylated by cytoplasmic phospholipase A2 to produce arachidonic acid. Arachidonic acid and its downstream products can promote tumor proliferation, invasion, and metastasis.[22] Sphingolipids are divided into sphingomyelins, sphingolipid sugars, and ceramides. Ceramides can be hydrolyzed by ceramidase to produce sphingosine, which can be converted into sphingosine-1-phosphate by sphingosine kinase, and sphingosine-1-phosphate can be converted into ceramide in reverse. Among them, ceramide and sphingosine inhibit cell growth and promotes cell apoptosis, whereas sphingosine-1-phosphate has the opposite effect. When this balance is disrupted, the normal apoptotic mechanism of cells is disturbed due to a decrease in ceramide content, thus promoting the development of tumors.[23]

In previous studies, Nam et al (2021) found[24] that most lipid levels in patients with CIN2/3 or cervical cancer were higher than those in healthy controls and patients with CIN1. The total Principal component (PC) and PE content showed a downward trend. These results indicate that changes in lipid metabolism, especially PC, PE, DG, and FFA, may affect the development of cervical cancer and that this unbalanced lipid metabolism remains unchanged in patients with cervical cancer. Cheng F et al (2020) showed[25] that the combination of PC (14:0/18:2), PE (15:1e/22:6), and PE (16:1e/

18:2) can be used as a promising serum biomarker to distinguish early precancerous lesion from squamous intraepithelial lesion (SIL) and healthy participants. Qi L et al (2023) showed[26] among different cervical cancer prognoses with low and high selenium levels six differential metabolites: glycylproline, PE[20:0/22:6(4Z,7Z,10Z,13Z,16Z,19Z)], 10-hydroxy -2E,8E-Decadiene-4,6-diynoic acid, 3-carboxy-4-methyl-5-propyl-2-furanpropanoic acid (CMPF), PC[20:5 (5Z,8Z,11Z,14Z,17Z)/P-18:1(11Z)], and 3-amino-octa-noic acid. Based on these six metabolites, the KEGG pathway analysis showed that glycerophosphate metabolism was the most significantly enriched pathway. Zhou H et al (2019) showed[27] that significant differences in the plasma metabolites PC (15:0/16:0), PG (12:0/13:0), LacCer (d18:1/ 16:0), d-maltose, and PA in patients with cervical squamous cell carcinoma (CSCC) with different prognoses. Zhou H et al (2020)[28] used 37 different metabolites for pathway analysis, and seven pathways were found to be enriched, among which sphingolipid and glycerophosphate metabolisms were significantly enriched (impact > 0.1). The area under the curve (AUC) values of eight metabolites were > 0.75 in each pair, namely ceramide [Cer (d18:1/16:0)], phosphatidylcholine [PC(15:0/16:0)], PC (16:0/16:0), phosphatidylethanolamine[PE (16:0/20:0)], PC (14:0/20:0), phosphatidylserine[PS (17:0/22:2(13Z,16Z))], phosphatidylglycerol [PG(21:0/22:4(7Z,10Z,13Z,16Z))] and sphingomyelin [SM (d18:1/20:0)]. These eight metabolites are phospholipids, and included six types of glycerophosphates and two types of sphingolipids, which enrich the metabolic pathways of glycerophosphates and sphingolipids, respectively. Hishinuma et al (2023) found[29] that compared with a healthy control group, the levels of 47 metabolites in patients with Uterine cervical cancer (UCC) were significantly increased, and the levels of 75 metabolites were significantly decreased. The characteristics of patients with UCC are increased arginine and ceramide levels and decreased tryptophan, ornithine, glycosylceramide, lysophosphatidylcholine, and phosphatidylcholine levels. Through joint pathway analysis, Yin et al found[30] that arachidonic acid and amino acid metabolisms are the most important pathways in cervical cancer. Amino acid and arachidonic acid metabolisms are the core metabolic pathways of naringin in HeLa cells. Li et al (2021) found[31] that phosphatidylserine, phosphatidylethanolamine, phosphatidylcholine, and sphingomyelin were downregulated by ZY0511. LSD1 plays a key role in lipid metabolism. Analysis of the lipid levels revealed different metabolic profiles among the four cancer cell lines. Although most lipids showed clear changes, sphingolipids and monoacylglycerols showed more pronounced changes. Liu et al (2023) showed[32] obvious differences between C33A and CaSki cells in metabolomics, especially in lipid metabolism.

The results showed that 1,2-dioleoyl-sn-glycerol-3-phosphate-L- serine, diglyceride, cerebroside B, PE-NMe(22:0/ 16:0), PE(18:2 (9z, 12z)/20:3 (5z, PE-NMe(16:1(9Z)/22:2(13Z, 16Z)), PE-NMe(20:0/16:0), linoleic acid, and methyl 15-cyano-pentadecanoate are decreased in cervical cancer. KEGG enrichment pathway showed that the most obvious enrichment pathway between cervical cancer and HPV-negative groups was steroid hormone pathway. MSEA showed that is the most important pathway in cervical cancer group compared with CIN2-3 and HPV-positive groups was sphingolipid metabolism pathway, followed by steroid biosynthesis and amino sugar and nucleotide metabolism pathways. Compared with the HPV-negative group, the most obvious enrichment pathway in the cervical cancer group was the steroid biosynthesis pathway, followed by the sphingolipid metabolism pathway. Thus, lipid metabolism plays an important role in the occurrence and development of cervical cancer.

Cervical Cancer and Amino Acid and Nucleotide Metabolic Pathways

Amino acids and their derivatives play important roles in several biochemical processes. Cervical cancer is closely related to the metabolism of amino acids and nucleotides. Hishinuma et al found[29] that compared with the healthy control group, the levels of cystine and arginine in patients with UCC increased significantly, whereas the levels of Trp, Orn, and lysoPC decreased significantly. Zhou et al (2023) found[33] that IGF-2BP3 stabilized the GLS and GLUD1 mRNAs; these are key metabolic enzymes involved in glutamine metabolism, thus glutamine metabolism is enhanced and production and release of lactic acid in tumor cells is promoted. These changes are helpful for Treg cell-mediated immune escape and identification of potential malignant tumors. Ran et al[34] compared cancer and control groups, and the area of eight common metabolites in hair and cervical tissue samples under the working characteristic curve of the participants was > 0.95. These metabolites are mainly involved in amino acid metabolism, cofactor synthesis, iron sag production, and glycolysis. Pappa et al (2021) found[19] that cervical cancer cells exhibit a distinct nucleic acid metabolism. The precursor of nucleotide synthesis is generated by pentose phosphate pathway (PPP), which converts the glycolytic intermediate

glucose-6-phosphate into gluconate-6-phosphate, and then into ribose-5-phosphate. HPV-related cells (SiHa and HeLa) showed significantly increased levels of the purine derivatives inosine and guanosine. Xu et al (2020) found[28] that the biosynthetic pathways of phenylalanine, tyrosine, and tryptophan (impact = 0.8, $P = 0.08$) changed in the progression of cervical cancer. Xu et al[35] used 155 different metabolites to enrich the KEGG pathway and found that the biosynthetic pathways of phenylalanine, tyrosine, and tryptophan are important in the occurrence of cervical cancer. Wang et al (2023) showed[36] that metabonomic pathway analysis revealed significant changes in the glutathione metabolic pathway of HeLa cells following Oridonin (Ori) treatment. Abudula at al. (2020) showed[37] that the levels of α- and β-glucose decreased, that of lactic acid and low-density lipoprotein increased, and the expression of various amino acids changed. This study showed that glutamine-glutamine-tryptophan, S-(4-methylthiobutylthiohydroxyacyl)-L-cysteine, ethyl-L-NIO, and other substances showed decreasing trends in cervical cancer. Compared with CIN2-3 and HPV-positive groups, the most obvious enrichment pathways in the cervical cancer group were the amino sugar and nucleotide sugar metabolism pathways. This shows that amino sugar and nucleotide sugar metabolic pathways play important roles in the occurrence and development of cervical cancer.

Conclusion

In this study, all the differential metabolites in the development of cervical cancer were detected by non-targeted metabolomics analysis, among which lipid metabolism was found to be the most important metabolic pathway in cervical cancer; amino acid and nucleotide metabolisms are also involved. The expression levels of 19-Hydroxytestosterone, cerebroside B, potassium acetate and methylarsonate are downregulated with the aggravation of cervical lesions and can be used as potential tumor markers for cervical cancer.

Data Sharing Statement

The data in this study are authentic and reliable. The datasets generated and/or analyzed for this study are not publicly available owing to patient privacy concerns; however, they can be accessed upon reasonable request from the corresponding authors.

Ethics Approval and Consent to Participate

The study adhered to ethical standards, and all participants provided written informed consent. We confirm that all procedures were conducted in accordance with the Cervical Cancer Clinical Practice Guidelines published by the National Comprehensive Cancer Network (NCCN). The study complied with the Declaration of Helsinki and received approval from the Ethics Committee of the Third Affiliated Hospital of Kunming Medical University (KYCS2021192).

Acknowledgments

We are grateful to the Yunnan Cancer Center for offering precious investigation field and data resources for this research. We appreciate all the staff and volunteers who took part in the data collection. We also express our thanks to all the patients with cervical lesions who participated in the face-to-face questionnaire survey for their proactive cooperation and robust support.

Funding

This study was supported by grants from Joint Special Project of Kunming Medical University - General Project (202201AY070001-163) and the innovative research team of Yunnan Province (Grant No.: 202305AS350020).

Disclosure

The authors declare that there are no conflicts of interest in this work.

References

1. Vu M, Yu J, Awolude OA, Chuang L. Cervical cancer worldwide. *Curr Probl Cancer*. 2018;42(5):457–465. doi:10.1016/j.currproblcancer.2018.06.003

2. Voelker RA. Cervical cancer screening. *JAMA*. 2023;330(20):2030. doi:10.1001/jama.2023.21987
3. Lycke KD, Kahlert J, Petersen LK, et al. Untreated cervical intraepithelial neoplasia grade 2 and subsequent risk of cervical cancer: population based cohort study. *BMJ*. 2023;383(e075925). doi:10.1136/bmj-2023-075925
4. Wolf J, Kist LF, Pereira SB, et al. Human papillomavirus infection: epidemiology, biology, host interactions, cancer development, prevention, and therapeutics. *Rev Med Virol*. 2024;34(3):e2537. doi:10.1002/rmv.2537
5. Yuan Y, Cai X, Shen F, Ma F. HPV post-infection microenvironment and cervical cancer. *Cancer Lett*. 2021;497:243–254. doi:10.1016/j.canlet.2020.10.034
6. Molina MA, Steenbergen RDM, Pumpe A, Kenyon AN, Melchers WJG. HPV integration and cervical cancer: a failed evolutionary viral trait. *Trends Mol Med*. 2024;30(9):890–902. doi:10.1016/j.molmed.2024.05.009
7. Kyrgiou M, Moscicki AB. Vaginal microbiome and cervical cancer. *Semin Cancer Biol*. 2022;86(Pt 3):189–198. doi:10.1016/j.semcancer.2022.03.005
8. Bhattacharjee R, Das SS, Biswal SS, et al. Mechanistic role of HPV-associated early proteins in cervical cancer: molecular pathways and targeted therapeutic strategies. *Crit Rev Oncol Hematol*. 2022;174:103675. doi:10.1016/j.critrevonc.2022.103675
9. Sawaya GF, Saraiya M, Soman A, Gopalani SV, Kenney K, Miller J. Accelerating cervical cancer screening with human papillomavirus genotyping. *Am J Prev Med*. 2023;64(4):552–555. doi:10.1016/j.amepre.2022.10.014
10. Yang Y, Han A, Wang X, Yin X, Cui M, Lin Z. Lipid metabolism regulator human hydroxysteroid dehydrogenase-like 2 (HSDL2) modulates cervical cancer cell proliferation and metastasis. *J Cell Mol Med*. 2021;25(10):4846–4859. doi:10.1111/jcmm.16461
11. Kuehn BM. WHO launches global push to eliminate cervical cancer. *JAMA*. 2021;325(3):213. doi:10.1001/jama.2020.25668
12. Pinto AP, Crum CP. Natural history of cervical neoplasia: definingprogression and its consequence. *Clin Obstet Gynecol*. 2000;43(2):352–362. doi:10.1097/00003081-200006000-00015
13. Nicholson JK, Lindon JC. Systems biology. *Metabolomics Nature*. 2008;455(7216):1054–1056. doi:10.1038/4551054a
14. Chen A, Xu M, Chen J, et al. Plasma-based metabolomics profiling of high-risk human papillomavirus and their emerging roles in the progression of cervical cancer. *Biomed Res Int*. 2022;2022:6207701. doi:10.1155/2022/6207701
15. Ilhan ZE, Łaniewski P, Thomas N, Roe DJ, Chase DM, Herbst-Kralovetz MM. Deciphering the complex interplay between microbiota, HPV, inflammation and cancer through cervicovaginal metabolic profiling. *EBioMedicine*. 2019;44:675–690. doi:10.1016/j.ebiom.2019.04.028
16. Zhang Y, Wu X, Li D, et al. HPV-associated cervicovaginal microbiome and host metabolome characteristics. *BMC Microbiol*. 2024;24(1):94. doi:10.1186/s12866-024-03244-1
17. Godoy-Vitorino F, Ortiz-Morales G, Romaguera J, Sanchez MM, Martinez-Ferrer M, Chorna N. Discriminating high-risk cervical human papilloma virus infections with urinary biomarkers via non-targeted GC-MS-based metabolomics. *PLoS One*. 2018;13(12):e0209936. doi:10.1371/journal.pone.0209936
18. Cancer Genome Atlas Research Network; Albert Einstein College of Medicine; Analytical Biological Services. Integrated genomic and molecular characterization of cervical cancer. *Nature*. 2017;543(7645):378–384. doi:10.1038/nature21386
19. Pappa KI, George D. Metabolic rewiring is associated with HPV-specific profiles in cervical cancer cell lines. *Sci Rep*. 2021;11(1):17718. doi:10.1038/s41598-021-96038-8
20. Xu H, Liu L, Xu F, et al. Microbiome-metabolome analysis reveals cervical lesion alterations. *Acta Biochim Biophys Sin*. 2022;54(10):1552–1560. doi:10.3724/abbs.2022149
21. Fahy E, Cotter D, Sud M, Subramaniam S. Lipid classification, structures and tools. *Biochim Biophys Acta*. 2011;1811(11):637–647. doi:10.1016/j.bbalip.2011.06.009
22. Freitas DRS, Sousa DNLA. Odete SB, et al. Phosphatidylcholine-derived lipid mediators: the crosstalk between cancer cells and immune cells. *Front Immunol*. 2022;13768606. doi:10.3389/fimmu.2022.768606
23. Janneh AH, Atkinson C, Tomlinson S, Ogretmen B. Sphingolipid metabolism and complement signaling in cancer progression. *Trends Cancer*. 2023;9(10):782–787. doi:10.1016/j.trecan.2023.07.001
24. Nam M, Seo SS, Jung S, et al. Comparable plasma lipid changes in patients with high-grade cervical intraepithelial neoplasia and patients with cervical cancer. *J Proteome Res*. 2021;20(1):740–750. doi:10.1021/acs.jproteome.0c00640
25. Cheng F, Wen Z, Feng X, Wang X, Chen Y. A serum lipidomic strategy revealed potential lipid biomarkers for early-stage cervical cancer. *Life Sci*. 2020;260:118489. doi:10.1016/j.lfs.2020.118489
26. Qi L, Wang Y, Wang R, et al. Association of plasma selenium and its untargeted metabolomic profiling with cervical cancer prognosis. *Biol Trace Elem Res*. 2023;201(10):4637–4648. doi:10.1007/s12011-022-03552-5
27. Zhou H, Li Q, Wang T, et al. Prognostic biomarkers of cervical squamous cell carcinoma identified via plasma metabolomics. *Medicine*. 2019;98(26):e16192. doi:10.1097/MD.0000000000016192
28. Zhou H, Li Q, Wang T, et al. Exploring metabolomics biomarkers for evaluating the effectiveness of concurrent radiochemotherapy for cervical cancers. *Transl Cancer Res*. 2020;9(4):2734–2747. doi:10.21037/tcr.2020.02.49
29. Hishinuma E, Shimada M, Matsukawa N, et al. Identification of predictive biomarkers for diagnosis and radiation sensitivity of uterine cervical cancer using wide-targeted metabolomics. *J Obstet Gynaecol Res*. 2023;49(8):2109–2117. doi:10.1111/jog.15709
30. Yin Z, Hua X, Lu M. Integrated network pharmacology and metabolomics to dissect the mechanisms of naringin for treating cervical cancer. *Comb Chem High Throughput Screen*. 2024;27(5):754–764. doi:10.2174/1386207326666230504124030
31. Li Y, Qian X, Lin Y, et al. Lipidomic profiling reveals lipid regulation by a novel LSD1 inhibitor treatment. *Oncol Rep*. 2021;46(5):233. doi:10.3892/or.2021.8184
32. Liu X, Zhu Y, Huang S, et al. Multiomics analysis of metabolic heterogeneity in cervical cancer cell lines with or without HPV. *Front Oncol*. 2023;13:1194462. doi:10.3389/fonc.2023.1194462
33. Zhou T, Xiao Z, Lu J, Zhang L, Bo L, Wang J. IGF2BP3-mediated regulation of GLS and GLUD1 gene expression promotes treg-induced immune escape in human cervical cancer. *Am J Cancer Res*. 2023;13(11):5289–5305.
34. Ran R, Zhong X, Yang Y, et al. Metabolomic profiling identifies hair as a robust biological sample for identifying women with cervical cancer. *Med Oncol*. 2023;40(2):75. doi:10.1007/s12032-022-01848-z
35. Xu H, Liu M, Song Y, et al. Metabolomics variation profiling of vaginal discharge identifies potential targets for cervical cancer early warning. *Acta Biochim Biophys Sin*. 2022;54(10):1561–1565. doi:10.3724/abbs.2022133

36. Wang W, Zhang N. Oridonin inhibits Hela cell proliferation via downregulation of glutathione metabolism: a new insight from metabolomics. *J Pharm Pharmacol*. 2023;75(6):837–845. doi:10.1093/jpp/rgad025
37. Abudula A, Rouzi N, Xu L, Yang Y, Hasimu A. Tissue-based metabolomics reveals potential biomarkers for cervical carcinoma and HPV infection. *Bosn J Basic Med Sci*. 2020;20(1):78–87. doi:10.17305/bjbms.2019.4359